Available online at www.sciencedirect.com
ScienceDirect
Trans. Nonferrous Met. Soc. China 25(2015) 2181−2187
Transactions of Nonferrous Metals Society of China
www.tnmsc.cn

Effects of processing parameters on microstructure of semi-solid slurry of AZ91D magnesium alloy prepared by gas bubbling

Yang ZHANG, Guo-hua WU, Wen-cai LIU, Liang ZHANG, Song PANG, Wen-jiang DING

National Engineering Research Center of Light Alloy Net Forming and State Key Laboratory of Metal Matrix Composite, School of Materials Science and Engineering, Shanghai Jiao Tong University, Shanghai 200240, China

Received 21 July 2014; accepted 23 January 2015

Abstract: The semi-solid slurry of AZ91D magnesium alloy was prepared by gas bubbling process. The effect of processing parameters, including gas flow rate, cooling rate and stirring end temperature, on microstructure of AZ91D semi-solid slurry was investigated. With increasing the gas flow rate from 0 to 5 L/min, the average size of primary α-Mg particles decreases from 119.1 to 77.2 μm and the average shape factor increases continuously from 0.1 to 0.596. The formation of non-dendritic primary α-Mg particles during gas bubbling is the result of combined effects of dendrite fragmentation and copious nucleation. With increasing the cooling rate from 3.6 to 14.6 °C/min, the average particle size of primary α-Mg phase decreases from 105.0 to 68.1 μm while the average shape factor peaks at 9.1 °C/min. Both high and low cooling rates can induce dendritic growth of primary α-Mg particles. Changing the stirring end temperature from 590 to 595 °C has little effect on the average size and shape factor of primary α-Mg particles in AZ91D semi-solid slurry. The insensitivity of semi-solid microstructures to the stirring end temperature is attributed to the sufficient quantity of primary particles formed in the melt.

Key words: AZ91D magnesium alloy; semi-solid slurry; gas bubbling; microstructure

1 Introduction

Semi-solid metal (SSM) processing generally consists of two technologies, i.e., rheoforming and thixoforming. Compared with thixoforming, rheoforming possesses several advantages, such as no need to make feedstock, no need to reheat, and recyclability of scrap. Therefore, rheoforming has been recognized more promising than thixoforming in practical applications in recent years. An important factor of successful rheoforming is the preparation of high-quality semi-solid slurry [1,2]. Traditionally, such semi-solid slurry can be prepared by applying vigorous agitation during solidification, including mechanical stirring [3] and electromagnetic stirring [4]. However, these processes always involve complex equipment and high cost. In recent years, a number of simple and cheap processes have been invented, such as serpentine pouring channel [5], self-inoculation [6], direct and indirect ultrasonic vibration [7,8]. It is still of great interest to search for new simple methods to prepare semi-solid slurry at reduced cost.

Gas induced semi-solid (GISS) process is a newly developed technique in which the preparation of semi-solid slurry is achieved by applying gas bubbles as the medium to agitate a molten metal during the initial stage of solidification [9]. WANNASIN et al [10−12] proved that GISS process was capable of preparing fine semi-solid slurry of several Al alloys. They also found that GISS was well coordinated with die casting, squeeze casting and gravity casting. However, the research on the preparation of semi-solid slurry of Mg alloys by GISS is little. A systematic study of effects of gas bubbling processing parameters on semi-solid microstructure is scarce.

Due to its low density, excellent mechanical property, good castability and high corrosion resistance, AZ91D is the most widely used die casting Mg alloy in industry. AZ91D also proved to be a good semi-solid alloy due to its wide solidification range and low temperature sensitivity of solid fraction [13,14].

Foundation item: Project (51275295) supported by the National Natural Science Foundation of China; Projects (20120073120011, 20130073110052) supported by the Research Fund for the Doctoral Program of Higher Education of China
Corresponding author: Guo-hua WU; Tel: +86-21-54742630; Fax: +86-21-34202794; E-mail: ghwu@sjtu.edu.cn
DOI: 10.1016/S1003-6326(15)63830-4

Therefore, AZ91D is suitable for the study of preparation of semi-solid slurry of Mg alloys by GISS. In this study, AZ91D semi-solid slurry was prepared by applying gas bubbling. The effects of gas bubbling processing parameters on the microstructure of AZ91D semi-solid slurry were examined. The mechanism of microstructure evolution of AZ91D semi-solid slurry during gas bubbling was discussed.

2 Experimental

Figure 1 shows a schematic of equipment used for gas bubbling. The diffuser was made of stainless steel with thin through-holes in the surface. Ar gas could go through the pipeline and spray from the holes.

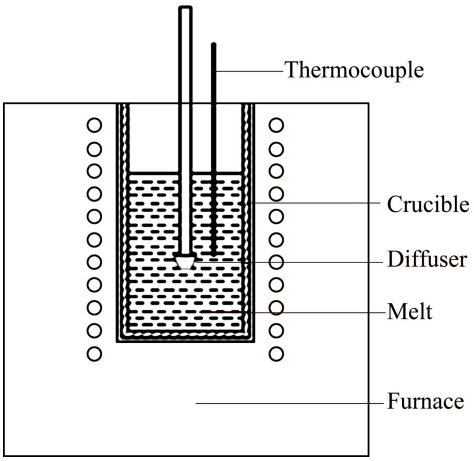

Fig. 1 Schematic of equipment used for gas bubbling

Commercial AZ91D alloy ingot was used in this study. The chemical compositions of AZ91D ingot were analyzed by ICP-AES. In each experiment, about 2 kg of AZ91D alloy was melted in a stainless steel crucible (d140 mm × 200 mm). A thermocouple was inserted into the melt to monitor and control the temperature. A protective atmosphere with a composition of $V(SF_6)$: $V(CO_2)$=1:100 was used to protect the melt from severe oxidation. After melting, the melt of AZ91D alloy was heated to 680 °C and held for 15 min. Then, the melt was transferred and cooled in the furnaces preheated to different temperatures, in order to achieve different cooling rates. When the melt was cooled down to 630 °C, the diffuser was quickly immersed into the melt, introducing Ar gas bubbles. The gas flow rate was controlled by the flow meter. When the predetermined stirring end temperature was arrived, the diffuser was removed. A slice of melt was quickly quenched in water when the temperature of melt reached 590 °C. To reveal the effects of processing parameters on the semi-solid microstructure, three parameters were taken into account, i.e., gas flow rate, cooling rate and stirring end temperature. Table 1 shows the details of experimental conditions.

Table 1 Processing parameters used in gas bubbling process

Variable parameter	Variable parameter value	Fixed parameter
Gas flow rate/ ($L \cdot min^{-1}$)	0	Cooling rate: 9.1 °C/min Stirring end temperature: 590 °C
	2	
	5	
Cooling rate/ ($°C \cdot min^{-1}$)	3.6	Gas flow rate: 5 L/min Stirring end temperature: 590 °C
	9.1	
	14.6	
Stirring end temperature/°C	590	Gas flow rate: 5 L/min Cooling rate: 9.1 °C/min
	595	

The water-quenched specimens were prepared with standard metallographic procedures. The microstructure characterization was carried out by optical microscopy (OM). The quantitative metallographic analysis was carried out using quantitative image analysis software. The quality of semi-solid slurry was evaluated with the size and roundness of primary α-Mg particles. The roundness of primary α-Mg particles is represented by the shape factor which is defined as $S_F=4\pi A/P^2$, where A and P represent the area and the perimeter of primary particles, respectively. The shape factor varies between 0 and 1, and S_F=1 indicates ideal circular.

3 Results

The chemical compositions of AZ91D ingot are listed in Table 2. Figure 2 shows the curve of solid fraction versus temperature of AZ91D ingot based on

Table 2 Chemical composition of AZ91D ingot (mass fraction, %)

Al	Zn	Mn	Mg
8.68	0.63	0.22	Bal.

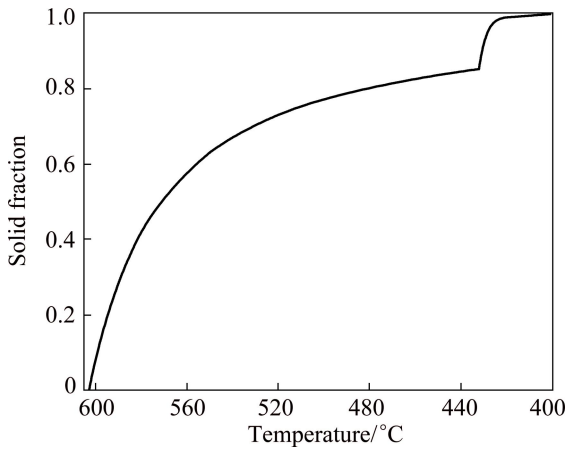

Fig. 2 Curve of solid fraction versus temperature of AZ91D alloy based on Scheil equation

Scheil equation, which was calculated with a commercial thermodynamic database software package called Pandat. As shown in Fig. 2, the primary α-Mg phase starts to form at 603.0 °C. The eutectic reaction appears at about 431.9 °C with the formation of β-$Mg_{17}Al_{12}$ phase. According to the calculation, the corresponding solid fraction of AZ91D at 590 °C is about 0.283. The average solid fraction analyzed from the quenched specimens by quantitative image analysis is about 0.316. Considering the inevitable secondary growth of primary particles during quenching [15], this result indicates that the calculation result of Pandat is credible.

3.1 Effect of gas flow rate on microstructure of AZ91D semi-solid slurry

Figure 3 shows the microstructures of as-quenched AZ91D semi-solid slurry samples prepared by gas bubbling under different gas flow rates. As shown in Fig. 3(a), when the melt is cooled to 590 °C without gas bubbling, the primary α-Mg particles show typically coarse dendritic morphology. When a gas flow rate of 2 L/min is introduced, the primary α-Mg particles become rosette-like and the size of primary α-Mg particles decreases dramatically. Further increasing the gas flow rate to 5 L/min, as shown in Fig. 3(c), the primary α-Mg particles grow rounder and disperse more uniformly.

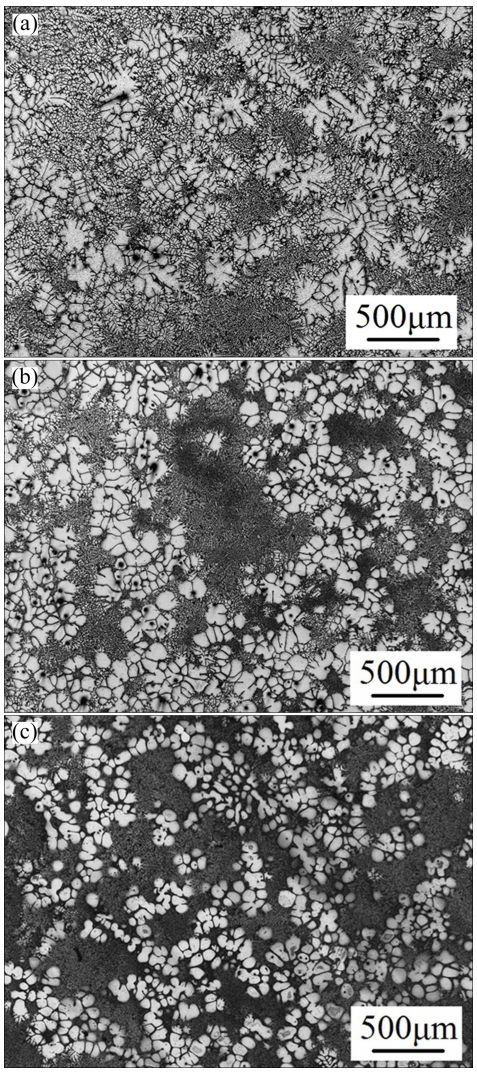

Fig. 3 Optical microstructures of AZ91D semi-solid slurry prepared by gas bubbling under different gas flow rates: (a) 0; (b) 2 L/min; (c) 5 L/min

The quantitative metallographic analysis results of average size and shape factor of primary α-Mg particles in AZ91D semi-solid slurry prepared by gas bubbling are illustrated in Fig. 4. With increasing the gas flow rate from 0 to 5 L/min, the solid fraction in as-quenched AZ91D semi-solid slurry samples does not change very much, varying from 0.312 to 0.305. It can be seen that, the average size of primary α-Mg particles decreases from 119.1 to 84.0 μm when the gas flow rate increases from 0 to 2 L/min and slightly decreases to 77.2 μm when the gas flow rate further increases to 5 L/min. With increasing the gas flow rate, the average shape factor of primary α-Mg particles increases continuously from 0.1 to 0.206 and then to 0.596. It is interesting that notable changes of primary α-Mg particle size and shape factor occur in different stages during the increase of gas flow rate. It is indicated from the quantitative analysis results that, if the gas flow rate increases to a higher degree, further refinement would be little although the primary α-Mg particles may become more spherical. During practical experiments, it is found that the gas flow rate higher than 5 L/min is easy to cause melt splashing during the gas bubbling process. Therefore, a gas flow rate of 5 L/min is chosen in following experiments.

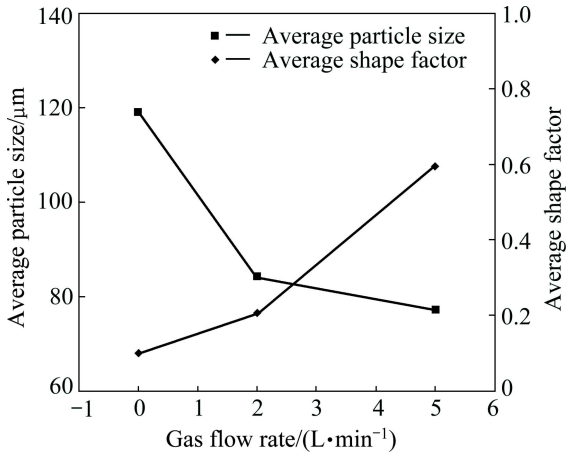

Fig. 4 Effect of gas flow rate on average size and shape factor of primary α-Mg particles in AZ91D semi-solid slurry

It is well accepted that increasing the stirring intensity can improve the quality of semi-solid slurry in SSM processing. In this study, as gas bubbling plays the role of agitating the melt, the increase of gas flow rate means the increase of stirring intensity. WANNASIN et

al [9] found that the gas flow rate had strong influences on the effectiveness of grain refinement. When the gas flow rate increased from 1 to 2 L/min, the grain refinement efficiency, which was defined as the fraction of non-dendritic microstructure, increased from 28% to about 56%. The result of this study is consistent with their conclusion. With increasing the gas flow rate, the quality of semi-solid slurry is significantly improved.

3.2 Effect of cooling rate on microstructure of AZ91D semi-solid slurry

In order to reveal the effect of cooling rate on the microstructure of AZ91D semi-solid slurry prepared by gas bubbling, the melt was transferred into furnaces separately pre-heated to 600, 500 and 300 °C to achieve different cooling rates. The corresponding cooling rates were 3.6, 9.1 and 14.6 °C/min, respectively. Figure 5 shows the microstructures of AZ91D semi-solid slurry specimens quenched at 590 °C under different cooling rates. The corresponding quantitative analysis results are shown in Fig. 6.

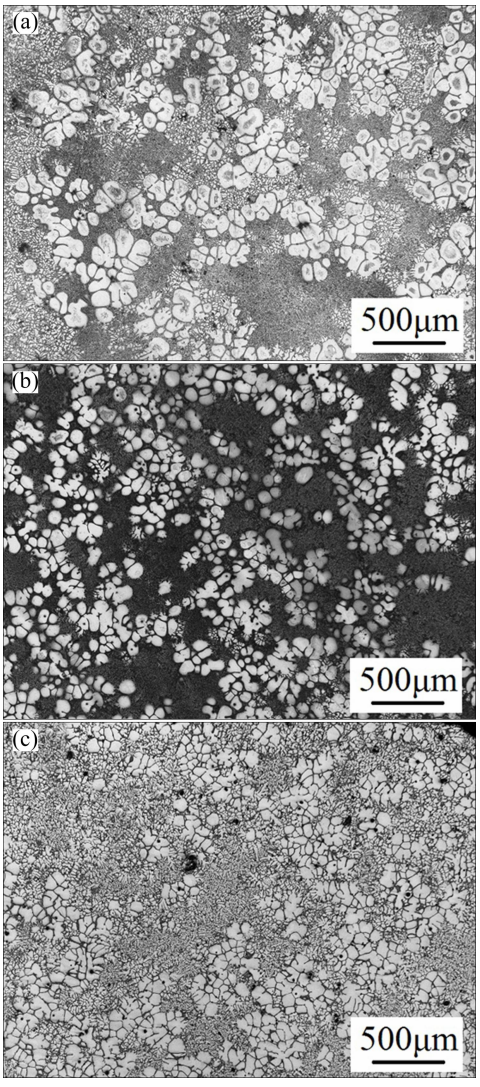

Fig. 5 Optical microstructures of AZ91D alloy slurry prepared by gas bubbling under different cooling rates: (a) 3.6 °C/min; (b) 9.1 °C/min; (c) 14.6 °C/min

With increasing the cooling rate from 3.6 to 14.6 °C/min, the solid fraction in as-quenched AZ91D semi-solid slurry samples significantly decreases from 0.352 to 0.305 and then 0.250. As shown in Fig. 5(a), when cooling at the rate of 3.6 °C/min, the primary α-Mg particles are coarse and rosette-like. When cooling at the rate of 14.6 °C/min as shown in Fig. 5(c), the primary α-Mg particles are small and also rosette-like. With increasing the cooling rate, the primary α-Mg particles exhibit continuous refinement. The average particle size of primary α-Mg phase decreases from 105.0 to 68.1 μm (Fig. 6). However, the primary α-Mg particles prepared under 9.1 °C/min exhibit better roundness than the specimens prepared under 3.6 °C/min or 14.6 °C/min. Taking both size and roundness of primary α-Mg particles into consideration, cooling too fast or too slow is neither desirable and a medium cooling rate of 9.1 °C/min is appropriate.

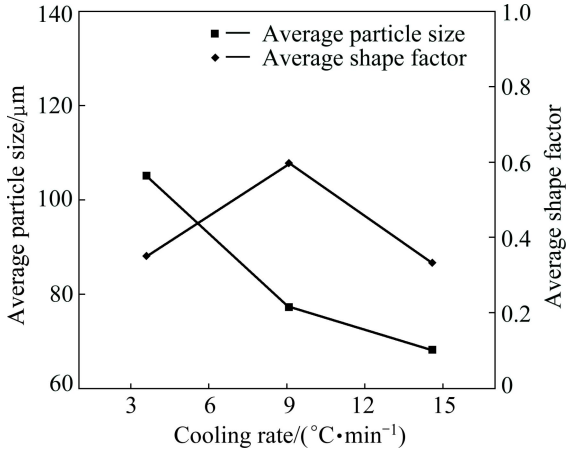

Fig. 6 Effect of cooling rate on average size and shape factor of primary α-Mg particles in AZ91D semi-solid slurry

3.3 Effect of stirring end temperature on microstructure of AZ91D semi-solid slurry

Figure 7 shows the microstructures of samples quenched at 590 °C with different stirring end temperatures. In Fig. 7(a), the sample was continuously stirred to 590 °C and then quenched in water immediately. In Fig. 7(b), the sample was stirred to 595 °C and quiescently cooled to 590 °C before quenching.

It is apparent in Fig. 7 that the change of stirring end temperature makes little difference on the microstructures of AZ91D semi-solid slurry. The quantitative analysis results of average grain size and shape factor of primary α-Mg particles in Fig. 8 show that, when the stirring end temperature changed from 590 to 595 °C, the average size of primary α-Mg particles slightly increases from 77.2 to 78.7 μm while the average

shape factor slightly increases from 0.596 to 0.621. The size distributions of primary α-Mg particles in Fig. 9 show that, although the size distribution of primary α-Mg particles in semi-solid slurry prepared at stirring end temperature of 595 °C becomes a little more uniform, there is no significant change in general trend when the stirring end temperature increased from 590 °C to 595 °C. The change of stirring end temperature also has little effect on the solid fraction. When the stirring end temperature changed from 590 °C to 595 °C, the solid fraction slightly increases from 0.305 to 0.321.

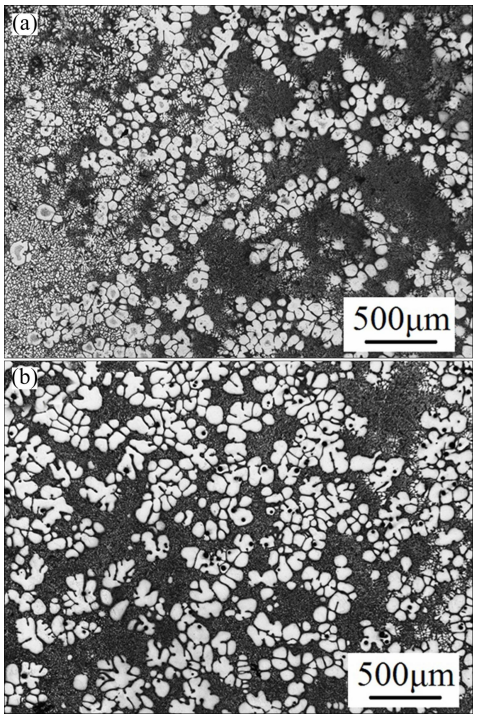

Fig. 7 Optical microstructures of AZ91D semi-solid slurry prepared by gas bubbling with different stirring end temperatures: (a) 590 °C; (b) 595 °C

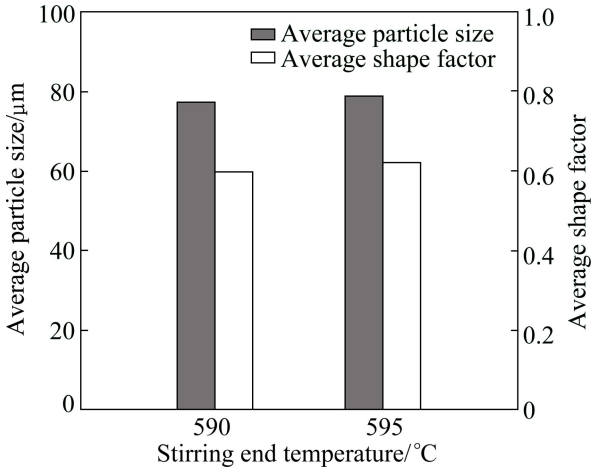

Fig. 8 Effect of stirring end temperature on average size and shape factor of primary α-Mg particles in AZ91D semi-solid slurry

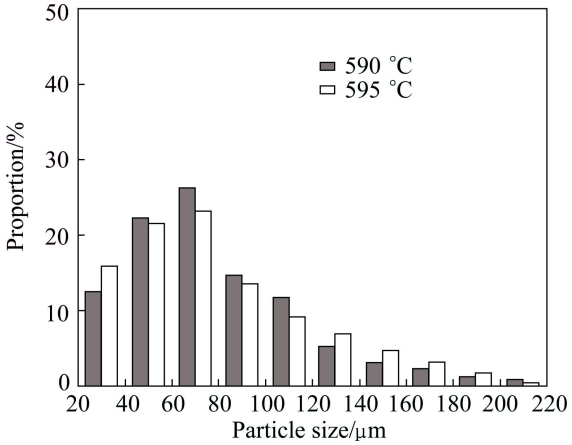

Fig. 9 Effect of stirring end temperature on size distribution of primary α-Mg particles in AZ91D semi-solid slurry

The increase of stirring end temperature is of practical value. With increasing the stirring end temperature, the time needed for gas bubbling and the consumption of gas are both reduced. In next study, higher stirring end temperatures will be attempted on the premise of causing no adverse effect to the quality of semi-solid slurry.

4 Discussion

4.1 Formation of non-dendritic primary α-Mg particles

Two theories are often proposed to explain the formation mechanism of numerous primary particles, i.e., copious nucleation and dendrite fragmentation. CANYOOK et al [16,17] studied the semi-solid microstructure evolution during the early solidification stages in GISS. They suggested that the fragmentation of dendrites by remelting was responsible for the formation of non-dendritic microstructure. In this study, another important factor that should not be ignored is the localized chilling achieved by gas flow. The primary particles may also form directly due to the localized chilling. For example, in the SSR process [18], a Cu rod was immersed into the melt and numerous primary particles were formed near the rod because of the highly localized chilling. In this study, since the temperature of Ar gas introduced into the melt is always lower than that of the melt itself, the introduction of Ar gas could induce both localized chilling and forced stirring in the melt during the gas bubbling process. The intensity of localized chilling and stirring is mainly determined by the level of gas flow. When the gas flow is at a high level, the localized chilling could be achieved effectively around the diffuser. Heterogeneous nucleation is likely to take place continuously in the undercooled region. Then, the formed nuclei would distribute homogeneously in the

melt driven by the gas flow. Moreover, due to the presence of the intensive forced stirring induced by gas bubbling, uniform temperature and concentration fields are created in the melt. DONG et al [19] concluded that uniform temperature and concentration fields had a favorable effect on the non-dendritic growth of primary particles. However, when the gas flow was at a low level, the amount of formed nuclei was insufficient and the stirring intensity was also limited, which led to the dendritic growth of some primary α-Mg particles. In this study, the formation of non-dendritic primary α-Mg particles during gas bubbling is the result of combined effects of dendrite fragmentation and copious nucleation.

4.2 Influence of cooling rate

According to classical solidification theory, the cooling rate has great effect on conventional solidification pattern. In the SSM processing, it has also been proven that the increase of cooling rate can significantly refine the primary particles [20]. The refinement of primary particles at high cooling rate is achieved by the promotion of nucleation and the restriction of growth. A relatively high cooling rate can promote the formation of primary particles by enhancing heterogeneous nucleation. The survival chance of formed nuclei can also increase due to the rapid release of latent heat. In addition, the high cooling rate shortens the growth time available for reaching the predetermined solid fraction, and restricts the growth of primary particles after nucleation. It is also found that, the increase of cooling rate promotes the continuous refinement of primary particles.

Simulative and experimental results show that, although the increase of cooling rate can bring about the refinement of primary phase, the roundness of particles worsens at the same time [21]. In this study, the worsening of roundness at high cooling rate is in accordance with the expectation because the high cooling rate can promote constitutional undercooling and induce instability of solid/liquid interface. However, the abnormal worsening of roundness at low cooling rate may be due to the loss of stability caused by excessive coarsening. According to the Mullins−Sekerka stability criterion, the primary particles would exhibit a perturbed periphery when growing to a certain size. Then, these particles would lose spherical morphology and develop into rosette-like or dendritic morphology during further growth. In the previous work, it was measured that the critical grain size of primary α-Mg particles is about 74 μm [22]. In this study, the average particle size when cooled at 3.6 °C/min is as large as 105.0 μm. Therefore, it is reasonable to assume that the primary α-Mg particles cooled at low cooling rate are easy to be perturbed and lose the stability.

4.3 Insensitivity of stirring end temperature

The insensitivity of semi-solid microstructures to the stirring end temperature was also reported by REISI and NIROUMAND [23]. They attributed this phenomenon to the sufficient quantity of primary particles formed in the melt. It is now accepted that when the density of primary particles is high enough, the space for the growth of these particles would be limited and the probability of overlap of diffusion fields of the adjacent particles would increase. As a result, the concentration gradient in front of solid–liquid interface would decrease and the interface stability would increase [24,25]. Under such condition, the prolongation of stirring will have little effect on the microstructure of AZ91D semi-solid slurry.

5 Conclusions

1) Increasing the gas flow rate from 0 to 5 L/min promotes significant refinement in the primary α-Mg particles and improvement of the roundness. The average size of primary α-Mg particles decreases from 119.1 to 77.2 μm and the average shape factor increases continuously from 0.1 to 0.596. The formation of non-dendritic primary α-Mg particles during gas bubbling is the result of combined effects of dendrite fragmentation and copious nucleation.

2) Increasing the cooling rate from 3.6 to 14.6 °C/min brings continuous refinement in the primary α-Mg particles while the roundness first increases and then decreases. The average particle size of primary α-Mg phase decreases from 105.0 to 68.1 μm. Both high and low cooling rates can induce dendritic growth of primary α-Mg particles.

3) Changing the stirring end temperature from 590 to 595 °C has little effect on the average size and shape factor of primary α-Mg particles in AZ91D semi-solid slurry. The insensitivity of semi-solid microstructures to the stirring end temperature is attributed to the sufficient quantity of primary particles formed in the melt.

References

[1] FLEMINGS M. Semi-solid forming: The process and the path forward [J]. Metallurgical Science and Technology, 2013, 18(2): 3−4.

[2] YOUNG K, EISEN P. SSM (semi-solid metal) technological alternatives for different applications [J]. Metallurgical Science and Technology, 2013, 18(2): 11−15.

[3] BOLOURI A, BAE J W, KANG C G. Tensile properties and microstructural characteristics of indirect rheoformed A356 aluminum alloy [J]. Materials Science and Engineering A, 2013, 562: 1−8.

[4] ZHANG L, LI W, YAO J P, QIU H. Effects of pulsed magnetic field on microstructures and morphology of the primary phase in semisolid A356 Al slurry [J]. Materials Letters, 2012, 66(1):

190−192.
[5] ZHU Wen-zhi, MAO Wei-min, TU Qin. Preparation of semi-solid 7075 aluminum alloy slurry by serpentine pouring channel [J]. Transactions of Nonferrous Metals Society of China, 2014, 24(4): 954−960.
[6] XING Bo, HAO Yuan, LI Yuan-dong, MA Ying, CHEN Ti-jun. Microstructure control of AZ31 alloy by self-inoculation method for semisolid rheocasting [J]. Transactions of Nonferrous Metals Society of China, 2013, 23(3): 567−575.
[7] ZHANG Liang, WU Guo-hua, WANG Shao-hua, DING Wen-jiang. Effect of cooling condition on microstructure of semi-solid AZ91 slurry produced via ultrasonic vibration process [J]. Transactions of Nonferrous Metals Society of China, 2012, 22(10): 2357−2363.
[8] LIN C, WU S, LV S, AN P, WAN L. Microstructure and mechanical properties of rheo-diecast hypereutectic Al−Si alloy with 2% Fe assisted with ultrasonic vibration process [J]. Journal of Alloys and Compounds, 2013, 568: 42−48.
[9] WANNASIN J, MARTINEZ R, FLEMINGS M. Grain refinement of an aluminum alloy by introducing gas bubbles during solidification [J]. Scripta Materials, 2006, 55(2): 115−118.
[10] WANNASIN J, JANUDOM S, RATTANOCHAIKUL T, CANYOOK R, BURAPA R, CHUCHEEP T, THANABUMRUNGKUL S. Research and development of gas induced semi-solid process for industrial applications [J]. Transactions of Nonferrous Metals Society of China, 2010, 20(S3): s1010−s1015.
[11] THANABUMRUNGKUL S, JANUDOM S, BURAPA R, DULYAPRAPHANT P, WANNASIN J. Industrial development of gas induced semi-solid process [J]. Transactions of Nonferrous Metals Society of China, 2010, 20(S3): s1016−s1021.
[12] CHUCHEEP T, BURAPA R, JANUDOM S, WISUTMETHANGOON S, WANNASIN J. Semi-solid gravity sand casting using gas induced semi-solid process [J]. Transactions of Nonferrous Metals Society of China, 2010, 20(S3): s981−s987.
[13] LIU Y, DAS A, FAN Z. Thermodynamic predictions of Mg−Al−M (M=Zn, Mn, Si) alloy compositions amenable to semisolid metal processing [J]. Materials Science and Technology, 2004, 20(1): 35−41.
[14] XIA M, HUANG Y, CASSINATH Z, FAN Z. Continuous twin screw rheo-extrusion of an AZ91D magnesium alloy [J]. Metallurgical and Materials Transactions A, 2012, 43(11): 4331−4344.
[15] REISI M, NIROUMAND B. Growth of primary particles during secondary cooling of a rheocast alloy [J]. Journal of Alloys and Compounds, 2009, 475(1−2): 643−647.
[16] CANYOOK R, PETSUT S, WISUTMETHANGOON S, FLEMINGS M C, WANNASIN J. Evolution of microstructure in semi-solid slurries of rheocast aluminum alloy [J]. Transactions of Nonferrous Metals Society of China, 2010, 20(9): 1649−1655.
[17] CANYOOK R, WANNASIN J, WISUTHMETHANGKUL S, FLEMINGS M. Characterization of the microstructure evolution of a semi-solid metal slurry during the early stages [J]. Acta Materials, 2012, 60(8): 3501−3510.
[18] MARTINEZ R, FLEMINGS M. Evolution of particle morphology in semisolid processing [J]. Metallurgical and Materials Transactions A, 2005, 36(8): 2205−2210.
[19] DONG J, CUI J, LE Q, LU G. Liquidus semi-continuous casting, reheating and thixoforming of a wrought aluminum alloy 7075 [J]. Materials Science and Engineering A, 2003, 345: 234−242.
[20] WU S, WU X, XIAO Z. A model of growth morphology for semi-solid metals [J]. Acta Materials, 2004, 52(12): 3519−3524.
[21] XU Jia, WU Guo-hua, LIU Wen-cai, ZHANG Yang, DING Wen-jiang. Effects of rotating gas bubble stirring treatment on the microstructures of semi-solid AZ91−2Ca alloy [J]. Journal of Magnesium and Alloys, 2013, 1(3): 217−223.
[22] QIAN M. Creation of semisolid slurries containing fine and spherical particles by grain refinement based on the Mullins–Sekerka stability criterion [J]. Acta Materials, 2006, 54(8): 2241−2252.
[23] REISI M, NIROUMAND B. Effects of stirring parameters on rheocast structure of Al−7.1 wt.% Si alloy [J]. Journal of Alloys and Compounds, 2009, 470(1−2): 413−419.
[24] GUO H, ZHANG A, HU B, DING Y, LIU X. Refining microstructure of AZ91 magnesium alloy by introducing limited angular oscillation during initial stage of solidification [J]. Materials Science and Engineering A, 2012, 532: 211−219.
[25] ZHANG Y, WU G, LIU W, ZHANG L, PANG S, DING W. Microstructure and mechanical properties of rheo-squeeze casting AZ91−Ca magnesium alloy prepared by gas bubbling process[J]. Materials & Design, 2015, 67: 1−8.

工艺参数对气泡搅拌法制备 AZ91D 镁合金半固态浆料显微组织的影响

张 扬，吴国华，刘文才，张 亮，庞 松，丁文江

上海交通大学 材料科学与工程学院，轻合金精密成型国家工程研究中心和
金属基复合材料国家重点实验室，上海 200240

摘 要：采用气泡搅拌法制备 AZ91D 镁合金半固态浆料，研究工艺参数变化，包括气体流量、冷却速率和搅拌结束温度，对 AZ91D 镁合金半固态浆料显微组织的影响规律。结果表明：随着气体流量从 0 升高至 5 L/min，α-Mg 初生相平均颗粒尺寸从 119.1 μm 降至 77.2 μm，而平均形状因子从 0.1 升高至 0.596，气泡搅拌中非枝晶初生相来自于枝晶破碎和熔体形核；随着冷却速率从 3.6 °C/min 升高至 14.6 °C/min，α-Mg 初生相平均颗粒尺寸从 105.0 μm 降至 68.1 μm，而平均形状因子在冷却速率为 9.1 °C/min 时达到最高，过高或过低的冷却速率都会导致初生相的枝晶生长；搅拌结束温度从 590 °C 升至 595 °C 对最终的 AZ91D 镁合金半固态浆料显微组织无明显影响，这是因为半固态浆料中已经形成了足够数量的初生相。

关键词：AZ91D 镁合金；半固态浆料；气泡搅拌；显微组织

(Edited by Mu-lan QIN)